

## Cross sections for electron scattering by atomic potassium

Alfred Z. Msezane, Paul Awuah, and Stephen Hiamang

*Department of Physics, Clark Atlanta University, Atlanta, Georgia 30314*

*and Center for Theoretical Studies of Physical Systems, Clark Atlanta University, Atlanta, Georgia 30314*

F. K. A. Allotey

*University of Science and Technology, Kumasi, Ghana*

(Received 13 February 1992)

Electron elastic and collisional excitation cross sections from the ground state of potassium are calculated using the noniterative integral-equation method of Henry, Rountree, and Smith [Comput. Phys. Commun. **23**, 233 (1981)] in the electron energy range  $4 \leq E \leq 200$  eV. Configuration-interaction target wave functions that take account of correlation and polarization effects are used to represent the ground state and the six lowest excited states  $4p^2P^\circ$ ,  $5s^2S$ ,  $3d^2D$ ,  $5p^2P^\circ$ ,  $4d^2D$ , and  $6s^2S$ . Elastic and discrete excitation cross sections are obtained in a seven-state close-coupling (7CC) approximation. The 7CC elastic and excitation cross sections are compared and contrasted. Near threshold the elastic cross section dominates the resonance,  $4s^2S \rightarrow 4p^2P^\circ$ , and the sum of the other remaining excitation cross sections. Comparison of our total cross sections with some available experimental and theoretical data is also effected. The discrepancy between the recent measurement of the total cross section by Kwan *et al.* [Phys. Rev. A **44**, 1620 (1991)] on the one hand and other measurements near threshold on the other hand is explained.

PACS number(s): 34.80.Bm, 34.80.Dp, 34.40.+n, 34.50.Fa

### I. INTRODUCTION

Some transitions in Na and K are important in studies of chemically driven visible laser amplifiers using fast near-resonance energy transfer [1]. On the fundamental side, van der Waals forces and the Casimir force represent the limiting cases of cavity QED and the shifts of the alkali-metal resonance lines may be studied in the laboratory as a test of cavity QED [2]. Thus it is important to calculate accurately the cross sections for the various transitions in the alkali metals to guide measurements.

In this paper we are interested in determining, using the noniterative integral-equation method (NIEM) of Henry, Rountree, and Smith [3] the magnitudes of the cross sections for electron elastic scattering and excitation from the ground state to the levels  $4p^2P^\circ$ ,  $5s^2S$ ,  $3d^2D$ ,  $5p^2P^\circ$ ,  $6s^2S$ , and  $4d^2D$  of K. The purpose of the investigation is mainly twofold. First, we want to assess the importance of the virtual double-dipole mechanism [4] with regard to the dipole-forbidden transition  $4s^2S \rightarrow 3d^2D$ . The mechanism is expected to increase the population of the  $3d^2D$  state significantly because the dipole oscillator strengths for the transitions  $4s^2S \rightarrow 4p^2P^\circ$  and  $4p^2P^\circ \rightarrow 3d^2D$  are large, being 1.20 and 0.90, respectively. Second, a comparison of the relative magnitudes of the elastic, the resonance, and the sum of the rest of the excitation cross sections near threshold may lead to an understanding of the source of discrepancy between the recent total-cross-section measurement of Kwan *et al.* [5] on the one hand and the experimental data of Vuskovic and Srivastava [6], Kasdan, Miller, and Bederson [7], and Visconti, Slevin, and Rubin [8] on the

other hand. Should the elastic cross section be comparable to or even greater than the excitation cross section (the ionization cross section is small near threshold), then the above discrepancy could be explained because of the inability of the Kwan *et al.* [5] experiment to discriminate against the elastically scattered electrons near the forward direction.

Resonance excitation cross sections for electron scattering by ground-state K have been measured [8–13] and evaluated [14–16]. Phelps *et al.* [13] have measured various discrete excitation cross sections and have also performed some calculations that included a Born approximation and a 15-state close-coupling (15CC) approximation, although excluding exchange effects. Stein *et al.* [17] and Kwan *et al.* [5] have employed a beam transmission technique to measure total cross sections.

Glauber and Glauber-related [18] approximations have been used to compute total cross sections, while Walters [14,15] obtained total cross sections for K by adding elastic, resonance excitation, the sum of discrete excitation other than the resonance excitation, and ionization cross sections selected from existing theoretical and experimental data. Kwan *et al.* [5] have also constructed the “Walters-Phelps curve” for the total cross section by selecting appropriate values of the elastic, resonance, sum of other discrete excitations, excluding the resonance excitation, and ionization cross sections from Walters [14,15] and Phelps *et al.* [13]. At electron-impact energies of less than 9 eV the total cross sections of Collins, Bederson, and Goldstein [19], Karule [20], Karule and Peterkop [21], and Visconti, Slevin, and Rubin [8] agree reasonably well. However, these results differ considerably from those of Brode [22].

Sections I and II give, respectively, the Introduction and the Target Wave Functions. In Sec. III we present the Cross Sections, while the Summary and Discussion are given in Sec. IV.

## II. TARGET WAVE FUNCTIONS FOR K

The lowest five states of K are close together in energy and the oscillator strengths for the transitions  $4s^2S \rightarrow 4p^2P^\circ$ ,  $4p^2P^\circ \rightarrow 3d^2D$ , and  $5s^2S \rightarrow 5p^2P^\circ$  are significant, roughly of order unity. Consequently, a reasonably good calculation of the total cross section for electrons scattered by atomic K must include at least the five states  $4s^2S$ ,  $3p^2P^\circ$ ,  $3d^2D$ ,  $5s^2S$ , and  $5p^2P^\circ$ . Furthermore, Phelps *et al.* [13] have measured and contrasted various electron-impact excitation cross sections for K. The relative contribution to the total cross section by those states above the lowest seven have been found to be small. In our construction of the target states for K we considered the fact that for weakly ionized atomic systems and neutrals the accuracy of the calculated cross section depends sensitively upon the representation of the target wave functions and the strength of the couplings among the various channels.

In generating the configurational target wave functions for K, we used the Clementi and Roetti [23] ionic orbitals  $1s$ ,  $2s$ ,  $2p$ ,  $3s$ ,  $3p$ , and  $4s$  for  $K^+$  as a starting point. These were fixed and program CIV3 of Hibbert [24] was employed to generate the additional excited orbitals  $3d$ ,  $4p$ ,  $4d$ ,  $4f$ ,  $5s$ ,  $5p$ ,  $5d$ , and  $6s$  as well as the configurational eigenstates. The radial functions of the required orbitals are expressed as

$$P_{nl} = r^l \sum_{i=1}^n c_i r^i \exp(-\alpha_i r), \quad (1)$$

where  $n$  and  $l$  are, respectively, the principal and orbital angular momentum quantum numbers. For a given

TABLE I. Target states and configurations used in their CI expansion for K.

Target states	Configurations
$3p^6 4s^2 S$ ; $3p^6 5s^2 S$ ; $3p^6 6s^2 S$	$3s^2 3p^6 4s$ , $3s^2 3p^6 5s$ , $3s^2 3p^6 6s$ , $3s^2 3p^5 3d 4p$ , $3s^2 3p^5 3d 5p$ , $3s^2 3p^5 4p 4d$ , $3s^2 3p^5 4s 4p$ , $3s^2 3p^5 5s 5p$ , $3s^2 3p^5 4s 5p$ , $3s^2 3p^5 3d 4f$ , $3s^2 3p^5 4p 5d$ , $3s^2 3p^5 4p 5s$ , $3s^2 3p^5 4d 4f$ , $3s^2 3p^5 4d 5p$ , $3s^2 3p^5 5p 5d$
$3p^6 4p^2 P^\circ$ ; $3p^6 5p^2 P^\circ$	$3s^2 3p^6 4p$ , $3s^2 3p^6 5p$ , $3s^2 2p^5 3d 4s$ , $3s^2 3p^5 3d 5s$ , $3s^2 3p^5 4s 4d$ , $3s^2 3p^5 4s^2$ , $3s^2 3p^5 3d^2$ , $3s^2 3p^5 4p^2$ , $3s^2 3p^5 3d 4d$ , $3s^2 3p^5 4d 5s$ , $3s^2 3p^5 4p 4f$
$3p^6 3d^2 D$ ; $3p^6 4d^2 D$	$3s^2 3p^6 3d$ , $3s^2 3p^6 4d$ , $3s^2 3p^6 5d$ , $3s^2 3p^5 4s 4p$ , $3s^2 3p^5 3d 4p$ , $3s^2 3p^5 4p 4d$ , $3s^2 3p^5 5s 4p$ , $3s^2 3p^5 3d 4f$ , $3s^2 3p^5 4d 4f$ , $3s^2 3p^5 4s 4f$
$3p^6 4f^2 F^\circ$	$3s^2 3p^6 4f$ , $3s^2 3p^5 3d^2$ , $3s^2 3p^5 4p^2$ , $3s^2 3p^5 4p 4f$ , $3s^2 3p^5 3d 4d$ , $3s^2 3p^5 3d 4s$ , $3s^2 3p^5 4s 4d$

TABLE II. Comparison of the present calculated  $\Delta E^P$  and experimental [26]  $\Delta E^E$  energy splittings (in a.u.) for the lowest eight states of K.

No.	State	$\Delta E^E$	$\Delta E^P$
1	$3p^6 4s^2 S$	0.0	0.0
2	$3p^6 4p^2 P^\circ$	0.059 34	0.051 42
3	$3p^6 5s^2 S$	0.095 81	0.085 92
4	$3p^6 3d^2 D$	0.098 13	0.088 56
5	$3p^6 5p^2 P^\circ$	0.112 61	0.101 19
6	$3p^6 4d^2 D$	0.124 84	0.114 60
7	$3p^6 6s^2 S$	0.125 08	0.116 86
8	$3p^6 4f^2 F^\circ$	0.128 16	0.118 04

choice of the exponents  $\alpha_i$  the expansion coefficients  $c_i$  are uniquely determined from the orthogonality condition

$$\int_0^\infty P_{nl}(r) P_{n'l}(r) dr = \delta_{nn'}. \quad (2)$$

The  $3d$ ,  $4p$ ,  $4d$ ,  $4f$ ,  $5s$ ,  $5p$ , and  $6s$  considered as spectroscopic orbitals were optimized on the states  $3p^6 3d^2 D$ ,  $3p^6 4p^2 P^\circ$ ,  $3p^6 4d^2 D$ ,  $3p^6 4f^2 F^\circ$ ,  $3p^6 5s^2 S$ ,  $3p^6 5p^2 P^\circ$ , and  $3p^6 6s^2 S$ , respectively, while the  $5d$  orbital may be viewed as a correlation-type orbital. The dominant eigenstates of potassium were constructed such that the oscillator strengths in the length  $f_L$  and velocity  $f_V$  formulations for the transitions of interest here were almost the same and consistent with accepted values [25]. Additionally, we require that the energy splittings between the ground state and the various excited states be compatible with the experimental values [26].

Table I presents the dominant eigenstates of K, from which the appropriate eigenstates were selected, and the corresponding configurations used. In Table II the present energy splittings,  $\Delta E^P$  are compared with the experimental values,  $\Delta E^E$  of Moore [26]. All but one of the calculated energy splittings are within 10% of the experimental ones.

Some oscillator strengths calculated from our eigenstates are compared in Table III with those of Wiese, Smith, and Miles [25]. The important length and velocity

TABLE III. Oscillator strengths in the length  $f_L$  and velocity  $f_V$  formulations for some dipole-allowed transitions in K. The values represented by  $f$  are from Wiese, Smith, and Miles [25].

Transition	$f_L$	$f_V$	$f$
$4s-4p$	1.075	1.037	1.020
$4s-5p$	0.005	0.008	0.009
$5s-4p$	0.183	0.171	0.183
$5s-5p$	1.507	1.497	1.500
$6s-4p$	0.013	0.010	0.020
$3d-4p$	0.931	0.973	0.900
$3d-5p$	0.162	0.184	0.140
$3d-4f$	1.104	1.186	0.750
$4p-4d$	0.013	0.022	0.051
$5p-4d$	1.290	1.245	1.200
$4d-4f$	0.251	0.148	0.350

TABLE IV. Clementi-type coefficients  $c_i$  and exponents  $\alpha_i$  for some orbitals of K, expressed in the form  $P_{nl}(r) = r^i \sum_{i=1}^n c_i r_i \exp(-\alpha_i r)$ .

$nl$	$i$	1	2	3	4	5	6
4s	$\alpha_i$	14.336 91	6.567 38	3.298 48	0.896 03		
	$c_i$	0.025 52	-0.093 53	0.199 33	-1.004 20		
5s	$\alpha_i$	14.336 91	6.567 38	3.298 48	0.896 03	0.462 73	
	$c_i$	0.010 03	-0.036 79	0.078 77	-0.438 77	1.091 29	
6s	$\alpha_i$	14.336 91	6.567 38	3.298 48	0.896 03	0.462 73	0.227 42
	$c_i$	0.003 13	-0.011 46	0.024 56	-0.138 71	0.395 48	-1.063 83
4p	$\alpha_i$		7.895 66	2.789 66	0.658 00		
	$c_i$		0.038 57	-0.122 80	1.001 00		
5p	$\alpha_i$		7.895 66	2.789 66	0.658 00	0.371 45	
	$c_i$		0.018 80	-0.060 07	0.542 92	-1.137 61	
6p	$\alpha_i$		7.895 66	2.789 66	0.658 00	0.371 45	0.325 61
	$c_i$		0.020 32	-0.065 12	0.626 87	-2.345 69	2.343 88
$nl$	$i$	3	3	3	4	4	5
3d	$\alpha_i$	7.090 21	4.176 30	2.664 75	0.456 56	1.085 03	
	$c_i$	0.005 78	-0.010 41	0.070 91	0.909 01	0.165 63	
4d	$\alpha_i$	0.404 65			0.209 97		
	$c_i$	0.536 96			-1.113 31		
5d	$\alpha_i$	0.314 28			0.187 97		0.236 34
	$c_i$	0.416 10			-12.126 72		11.812 16
4f	$\alpha_i$				0.214 28		
	$c_i$				1.000 00		

oscillator strengths, corresponding to the transitions  $4s \rightarrow 4p$ ,  $5s \rightarrow 5p$ ,  $3d \rightarrow 4p$ , and  $5p \rightarrow 4d$  are in reasonable accord with each other and are within 6% of the values of Wiese, Smith, and Miles [25]. Note that the small-valued oscillator strengths are given with large uncertainty by Wiese, Smith, and Miles [25] and the purpose here is to construct a reasonably good wave function for K using  $f$  values as a guide. The Clementi-type coefficients and the exponents of the generated orbitals are given in Table IV.

### III. CROSS SECTIONS

The noniterative integral-equation method of Henry, Rountree, and Smith [3] was used to solve the integro-differential equations that arise in the close-coupling approximation and to obtain the electron elastic and discrete excitation cross sections for K. In the calculation, the basic step size at small values of  $r$ , the radial distance, is  $0.0017a_0$ , where  $a_0$  is the Bohr radius. At  $r = 30.3a_0$  exchange terms were neglected because the longest-ranged orbital had fallen to less than  $10^{-3}$ . Bound configurations were generated by keeping fully occupied the  $1s$  through  $3p$  and the  $4s$  orbitals, while the remaining orbitals were each allowed only single occupation. A large number of configurations was thus generated, particularly for small impact energies and small orbital angular momentum values  $L \leq 5$ . This necessitated the omission of coefficients in the expansion terms of less than 0.02. The NIEM cross sections were checked against those from the  $R$ -matrix code of Berrington *et al.*

[27] at 4, 6, and 10 eV, in which the  $R$ -matrix boundary radius was taken to be  $30.3a_0$ . The two procedures agreed very well on the sum of the partial cross sections for  $L = 0$  to 5 but not on the individual partial cross sections. The agreement satisfied us because the objective of this calculation is to evaluate summed partial cross sections for the various transitions from the ground state of K.

The close-coupling equations were solved using Program NIEM for values of  $L$  up to 24. From  $L = 25$  to the highest partial waves, the cross sections for the optically allowed transitions were evaluated using the Bethe procedure. Only the elastic and excitation cross sections are computed by Program NIEM. Consequently, we use ionization cross sections  $\sigma_I$  obtained by others [14,15] to achieve the total cross sections  $\sigma_T$  for comparison with measurements and other calculations. The ionization cross sections are generally small in the energy range of interest of this paper, varying from 0 to about  $4.4 \times 10^{-16} \text{ cm}^2$ . Their contribution to the total cross section is relatively small, particularly near threshold where the recent measurement [5] deviates significantly from most existing experimental measurements and theoretical calculations.

Table V presents our calculated 7CC elastic and excitation cross sections, all in units of  $\pi a_0^2$ , in the electron energy range  $4 \leq E \leq 200 \text{ eV}$ . We have labeled the cross sections consistent with the numbering of the states in Table II, viz.,  $\sigma_1, \sigma_2, \sigma_3, \sigma_4, \sigma_5, \sigma_6$ , and  $\sigma_7$ , corresponding to the cross sections for the transition from the ground state to  $4s^2S, 4p^2P^\circ, 5s^2S, 3d^2D, 5p^2P^\circ, 4d^2D$ , and

TABLE V. Elastic and excitation cross sections (in units of  $\pi a_0^2$ ) for electron scattering by potassium as a function of electron energy (eV). The cross sections  $\sigma_1, \sigma_2, \sigma_3, \sigma_4, \sigma_5, \sigma_6$ , and  $\sigma_7$  represent cross sections from ground state to  $4s^2S, 4p^2P^o, 5s^2S, 3d^2D, 5p^2P^o, 4d^2D$ , and  $6s^2S$  states, respectively, while  $\sigma_8$  corresponds to excitation to  $4f^2F^o$  using a 2CC calculation. The sum of the eight cross sections is denoted by  $\sigma_s$ .

$E$ (eV)	$\sigma_1$	$\sigma_2$	$\sigma_3$	$\sigma_4$	$\sigma_5$	$\sigma_6$	$\sigma_7$	$\sigma_8$	$\sigma_s$
4	87.510	61.230	3.720	16.011	1.751	1.961	0.562	1.820	174.565
6	58.230	57.510	5.298	17.657	3.554	2.550	1.431	1.910	147.690
10	41.340	51.824	5.053	9.701	3.088	2.520	0.675	1.340	115.537
15	28.220	48.008	3.266	7.841	2.206	1.520	0.475	0.810	92.342
20	22.100	43.706	2.241	6.617	1.781	1.051	0.361	0.522	78.384
30	18.380	38.768	1.350	4.780	1.392	0.751	0.249	0.243	65.817
60	11.500	25.510	0.702	2.310	0.704	0.354	0.133	0.120	41.334
100	8.190	18.210	0.301	1.420	0.431	0.225	0.091	0.111	28.981
150	6.290	14.120	0.154	1.050	0.336	0.155	0.063	0.075	22.246
200	4.950	12.000	0.122	0.820	0.298	0.110	0.043	0.051	18.388

$6s^2S$ , respectively. For comparison, the 2CC cross section for the transition  $4s^2S \rightarrow 4f^2F^o$  has also been included in the column, labeled  $\sigma_8$ . The total electron-impact cross section,  $\sigma_T$  for K is obtained by adding all the columns of Table I at a given energy plus the ionization cross section  $\sigma_I$  estimated from the curve of Walters [15]. We note that the ionization cross section varies from 0 at 4 eV to about  $4.4 \times 10^{-16} \text{ cm}^2$  at 15 eV; at 100 eV it is approximately  $2.25 \times 10^{-16} \text{ cm}^2$ . In the energy region of major importance in this paper,  $4 \leq E \leq 10 \text{ eV}$ , it contributes a maximum of 3.7% to  $\sigma_T$ .

For convenience, we represent the cross sections for elastic and resonance scattering and the sum  $\sigma_{5s} + \sigma_{3d} + \sigma_{5p} + \sigma_{6s} + \sigma_{4d} + \sigma_{4f}$  by  $\sigma_E, \sigma_R$ , and  $\sigma_D$ , respectively. In Fig. 1 we compare the present  $\sigma_E$  (---),  $\sigma_R$  (····),  $\sigma_D$  (—), and  $\sigma_S$  (—··—), the sum of  $\sigma_E, \sigma_R$ , and  $\sigma_D$ , for the electron energy range  $4 \leq E \leq 100 \text{ eV}$ . Near threshold  $\sigma_E$  is the dominant cross section; it is even greater than  $\sigma_R$  but falls off more rap-

idly in comparison with it as the impact energy increases. Beyond about 30 eV,  $\sigma_E$  decreases at almost a constant slope such that  $\sigma_R > \sigma_E > \sigma_D$ . The behavior of  $\sigma_E$  relative to  $\sigma_R$  and  $\sigma_D$  near threshold has important consequences for the measurement of the total cross section by the method of Kwan *et al.* [5].

In Fig. 2 we contrast for  $4 \leq E \leq 60 \text{ eV}$  the various remaining discrete excitation cross sections, represented as  $\sigma_{5p}$  (---),  $\sigma_{3d}$  (····),  $\sigma_{5s}$  (----),  $\sigma_{4d}$  (—), and  $\sigma_{6s}$  (—··—). We note that the excitation cross section for the  $3d^2D$  state is large in comparison with the others. This may be understood in terms of the virtual-double-dipole mechanism [4], which causes the  $3d^2D$  state to be populated additionally through the transition  $4s^2S \rightarrow 4p^2P^o$  and  $4p^2P^o \rightarrow 3d^2D$ . This is due to the large oscillator strengths for these transitions, being 1.020 for the former and 0.900 for the latter. The same mechanism has been found to cause the  $3d^2D$  state of Na to behave like a dipole-allowed transition [30]. Similarly, the  $4d^2D$  state has a larger than expected population, again because of the virtual-double-dipole mechanism,

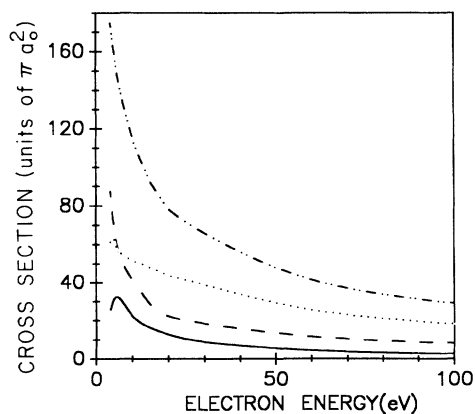


FIG. 1. Comparison of our calculated electron elastic  $\sigma_E$ , resonance  $\sigma_R$ , and sum of excitation other than the resonance  $\sigma_D$  cross sections (in units of  $\pi a_0^2$ ) for potassium vs electron-impact energy (eV), demonstrating their contribution to the sum  $\sigma_S$ . In the figure, ---, ····, —, and —··— represent  $\sigma_E, \sigma_R, \sigma_D$ , and  $\sigma_S$ , respectively.

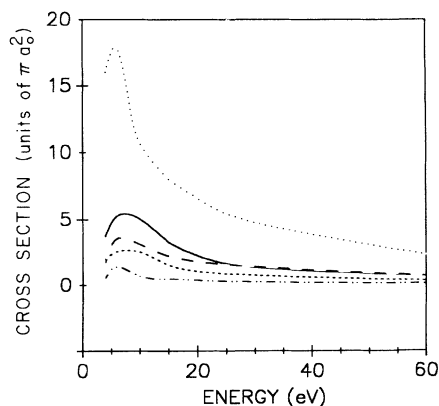


FIG. 2. Electron discrete excitation cross sections (in units of  $\pi a_0^2$ ) for K vs electron energy (eV). The curves ---, ····, ----, —, and —··— represent cross sections for the transitions  $4s^2S \rightarrow 5p^2P^o$ ,  $4s^2S \rightarrow 3d^2D$ ,  $4s^2S \rightarrow 5s^2S$ ,  $4s^2S \rightarrow 4d^2D$ , and  $4s^2S \rightarrow 6s^2S$ , respectively, in the 7CC approximation.

this time operating through  $5s^2S \rightarrow 5p^2P^\circ$  and  $5p^2P^\circ \rightarrow 4d^2D$ . The  $f$  values for these transitions are also large, being 1.500 and 1.200, respectively. Consequently, once the  $5s^2S$  or  $5p^2P^\circ$  state is populated, or both are populated, additional flux is then fed to the  $4d^2D$  level.

In calculating  $\sigma_T$  we have used the values in Table V and  $\sigma_I$ . The values recommended by Walters [15] have been used for  $\sigma_I$ , rather than those measured directly by Korchevoi and Prozonki [28] and McFarland and Kinney [29]. In Fig. 3 we compare total electron-impact cross sections from the present calculation with those measured by Kwan *et al.* [5], Vuskovic and Srivastava [6], Kasdan, Miller and Bederson [7], and Visconti, Slevin, and Rubin [8]. The constructed Walters and Phelps curve [5] and Gien's MG1 and MG3 results are also shown. All the total cross sections of Fig. 3 are in units of ( $10^{-16} \text{ cm}^2$ ).

In the energy region between about 15 and 50 eV there is significant discrepancy among the experimental measurements, while below 10 eV the measurements exhibit good agreement, except that the recent one by Kwan *et al.* [5] underestimates the others. Beyond about 45 eV the measurements of Vuskovic and Srivastava [6] and Kwan *et al.* are in reasonable agreement, but disagree strongly with the Kasdan, Miller, and Bederson [7] data. Near threshold, the Kwan *et al.* experiment measures the total cross section inaccurately because of the dominance of the elastic cross section over the others. This experiment [5] is unable to discriminate against the elastically scattered electrons near the forward direction.

The theoretical calculations, bounded below by MG1 and above by MG3, agree reasonably well for  $E$  greater than about 30 eV, with the present calculation showing

better agreement with the Walters-Phelps curve. The worst agreement is between Gien's MG1 and MG3 for  $E$  less than about 30 eV. Near threshold our calculation slightly overestimates both the measurements and the Walters-Phelps curve. A possible explanation for this is that in the 7CC calculation flux is artificially restricted to accumulate in the  $4d^2D$  state; the effect is apparently significant near threshold. We note that the oscillator strength for the  $5p^2P \rightarrow 4d^2D$  transition is large and equals 1.200. The inclusion of higher states in the present 7CC calculation could reduce our total cross sections through reduction of the inelastic ones. We believe that our elastic cross section is calculated accurately because a 5CC and a 2CC calculation, each containing the  $4p^2P^\circ$ , left the elastic cross section essentially the same.

In Fig. 4 we have contrasted the various experimental and theoretical data for the resonance excitation cross section (in units of  $\pi a_0^2$ ) in the electron energy interval  $1.5 \leq E \leq 100$  eV. As can be seen from Fig. 4, the Phelps *et al.* measurement is the only data that shows a minimum for  $\sigma_R$  in the interval  $2 \leq E \leq 10$  eV; all others do not.

Around the position of the maximum for  $\sigma_R$ , the various data are scattered wildly. They tend to approach one another very close to threshold and at high energy. Our  $\sigma_R$  values are lower than most, except the Vuskovic and Srivastava data. The reason for this is probably found in the target wave function, which gives the energy splitting between the ground and the resonance levels a value much lower than the experimental one, about 13%.

Note that the constructed Walters-Phelps curve by Kwan *et al.* uses the recommended elastic and ionization cross sections of Walters [15] and the experimental values of Phelps *et al.* [13] for the resonance and discrete excitation cross sections other than the resonance one. Interestingly, the measured [13] resonance cross section shows a dip between about 2 and 10 eV and has the

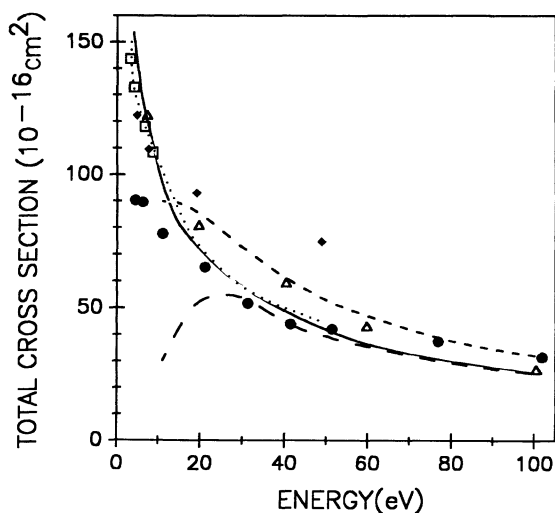


FIG. 3. Comparison of theoretical and experimental total electron-impact cross sections (in units of  $10^{-16} \text{ cm}^2$ ) vs electron energy (eV) for K. The theoretical results are present (—), Gien's MG1 (---), MG2 (— · —), and the constructed Walters-Phelps curve [5] (· · ·). The experimental data are from Kwan *et al.* [5] (●); Vuskovic and Srivastava [6] (△); Kasdan, Miller, and Bederson [7] (◆); and Visconti, Slevin, and Rubin [8] (□).

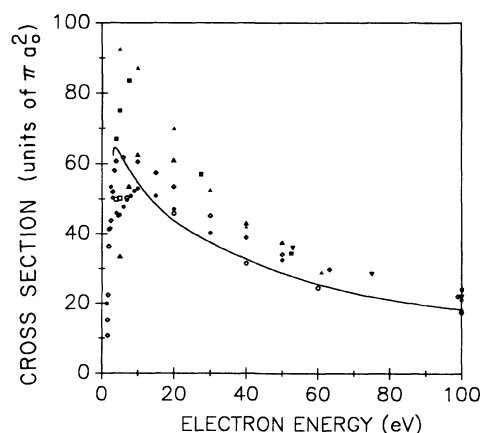


FIG. 4. Resonance cross sections (in units of  $\pi a_0^2$ ) for K. Experimental data: Chen and Gallagher [10] (◇); Phelps *et al.* [13] (●); Vuskovic and Srivastava [6] (○); Buckman, Noble, and Teubner [9] (▽); Zapesochnyi, Postoi, and Aleksakhin [12] (▲). Theory: Present —; Kennedy, Myerscough, and McDowell [16] (■); Walters [15] (△); and Moores [31] (□).

lowest value of about  $40 \times 10^{-16} \text{ cm}^2$  at about 4 eV. In this same energy interval, all other measurements [8–12] and calculations [14–16], including the present one, do not reveal this minimum. Consequently, if any other  $\sigma_R$  values other than the Phelps *et al.* data were used, the Walters-Phelps curve would add a value of between 0 and  $10 \times 10^{-16} \text{ cm}^2$  in the energy range  $2 \leq E \leq 10 \text{ eV}$ . In this energy interval the Walters-Phelps curve would then have much higher values than presented by Kwan *et al.*

Perhaps future calculations could concentrate in the energy region  $2 \leq E \leq 15 \text{ eV}$ , using a finer energy mesh than used here to determine the correct behavior of  $\sigma_R$ . The method of Moores and Norcross [32], which has been successful in another context, comes naturally. We have also compared some of our 7CC cross sections with the Born results of Phelps *et al.* [13] (results not shown). For the  $5s^2S$  and the  $6s^2S$  cross sections agreement is quite good for  $E > 40 \text{ eV}$  and  $E > 6 \text{ eV}$ , respectively, while for  $3d^2D$  agreement is remarkable for  $E > 10 \text{ eV}$ . The cross sections for  $4p^2P^\circ$  and  $5p^2P^\circ$  lead to the worst discrepancy just as for  $4d^2D$  in the energy interval  $4 \leq E \leq 40 \text{ eV}$ . Some of the agreements may be fortuitous, but for  $E \geq 100 \text{ eV}$  ( $E \geq 150 \text{ eV}$  for dipole-allowed transitions), where Born approximation is expected to be valid, agreement between the Born and our results is generally good. Comparing some of our 7CC cross sections with the 15CC values of Phelps *et al.* may be meaningless because the 15CC calculation neglected exchange effects in the energy region covered; this is where they are expected to be significant.

#### IV. SUMMARY AND DISCUSSION

We have calculated in a 7CC approximation cross sections for elastic scattering and discrete excitations of the lowest six states from ground state of K by electron impact in the energy range  $4 \leq E \leq 200 \text{ eV}$ . Additionally, a 2CC approximation has been employed to obtain the  $4f^2F^\circ$  cross section. Our total cross section, obtained by adding the 7CC values, the 2CC values, and the values of the ionization cross section recommended by Walters [15], has been compared with various measurements and theoretical calculations. Large discrepancies occur among the calculated and measured total cross sections in the approximate energy interval  $20 \leq E \leq 50 \text{ eV}$ . For  $E > 50 \text{ eV}$  agreement among the measurements [5,6], the current, and Gien's calculations is reasonably good. Near threshold there is a very good agreement among the measurements [6–8] and the Walters-Phelps curve [5]. However, the various theoretical calculations differ significantly, with the present calculation showing a better agreement with the Walters-Phelps curve. As pointed out in Sec. III, the measurement of Kwan *et al.* underestimates the total cross section due mainly to a large elastic cross-section component in  $\sigma_T$ , whose measurement causes some difficulties for the experiment of Kwan *et al.*

Near threshold our calculation overestimates slightly the measurements and the Walters-Phelps curve. This is

due probably to overestimation of some of the inelastic cross sections, particularly the  $4d^2D$  because of the termination of our calculation in the  $6s^2S$  state. This results in the accumulation of flux particularly in the  $4d^2D$  state because of the virtual-double-dipole mechanism, manifesting through the  $5s^2S-5p^2P^\circ$  and  $5p^2P^\circ \rightarrow 4d^2D$  transitions, seen from the large  $f$  values 1.500 and 1.200, respectively. The same mechanism is responsible for the additional population of the  $3d^2D$  state since the oscillator strengths for  $4s^2S \rightarrow 4p^2P^\circ$  and  $4p^2P^\circ \rightarrow 3d^2D$  are large, being 1.020 and 0.900, respectively; they cause the  $4s^2S \rightarrow 3d^2D$  to behave like a dipole-allowed transition.

A shortcoming with the close-coupling approximation as used here to calculate the total cross section is in its inability to evaluate directly the ionization cross section. However, its dependence upon  $\sigma_I$  obtained from others is less troublesome here because  $\sigma_I$  is small throughout the energy range considered in this paper; it contributes a maximum of about 3.7% to the total cross section at 10 eV. A problem, though not major, may arise from the artificial termination of the calculation at the  $6s^2S$  state. We checked our 7CC against our previous 5CC [33] data and found that  $\sigma_E$ ,  $\sigma_R$ , and  $\sigma_{3d}$  are insensitive to the additional  $6s^2S$  and  $4d^2D$  states; these are the major contributors to the total cross section in the region of interest of this paper.

Finally, we note that the Walters-Phelps curve [5] may be inappropriately constructed in the approximate interval  $2 \leq E \leq 10 \text{ eV}$  because of its use of the Phelps *et al.* values for the resonance cross section, which shows a minimum at around 4 eV. This may result in the underestimation of the total cross section of as much as  $10 \times 10^{-16} \text{ cm}^2$  at the minimum. All other measurements [8–12] and theoretical calculations [14–16], including the present one, do not reveal the minimum. We conclude by suggesting that the energy region  $2 \leq E \leq 15 \text{ eV}$  be examined very carefully using a finer energy mesh than used here to ascertain primarily the behavior of the resonance  $4p^2P^\circ$  cross section and hence the total cross section. The near-threshold energy region may be studied by the method of Moores and Norcross [32], which has been successful in another context.

#### ACKNOWLEDGMENTS

The research was supported in part by the U.S. Department of Energy, Office of Basic Energy Sciences, Division of Chemical Sciences, and the National Science Foundation. Dr. Allotey's visit to Clark Atlanta University was supported by a grant from the Office of Naval Research. Generous computer time is highly appreciated on the National Research Supercomputer Center Cray supercomputers from the Division of Chemical Sciences, Office of Basic Energy Sciences and Office of Fusion Energy, U.S. Department of Energy. We thank Dr. T. S. Stein for valuable discussions and keeping us informed about their measurements on K.

- [1] K. K. Shen, C. Winshead, and J. L. Gole, *Bull. Am. Phys. Soc.* **35**, 2359 (1990).
- [2] E. A. Hinds and V. Sandoghdan, in *Abstracts of Papers, Proceedings of the ICAP-12, Ann Arbor, Michigan, 1990*, edited by W. E. Baylis *et al.* (University of Michigan, Ann Arbor, 1990), p. I-27.
- [3] R. J. W. Henry, S. P. Rountree, and E. R. Smith, *Comput. Phys. Commun.* **23**, 233 (1981).
- [4] I. V. Hertel and K. A. Rost, *J. Phys. B* **4**, 690 (1971).
- [5] C. K. Kwan, W. E. Kauppila, R. A. Lukaszew, S. P. Parikh, T. S. Stein, Y. J. Wan, and M. S. Dababneh, *Phys. Rev. A* **44**, 1620 (1991).
- [6] L. Vuskovic and S. K. Srivastava, *J. Phys. B* **13**, 4849 (1980).
- [7] A. Kasdan, T. M. Miller, and B. Bederson, *Phys. Rev. A* **8**, 1562 (1973).
- [8] P. J. Visconti, J. A. Slevin, and K. Rubin, *Phys. Rev. A* **3**, 1310 (1971).
- [9] S. J. Buckman, C. J. Noble, and P. J. O. Teubner, *J. Phys. B* **12**, 3077 (1979).
- [10] S. T. Chen and A. C. Gallagher, *Phys. Rev. A* **17**, 551 (1978).
- [11] W. Williams and S. Trajmar, *J. Phys. B* **10**, 1955 (1977).
- [12] I. P. Zapesochnyi, E. N. Postoi, and I. S. Aleksakhin, *Zh. Eksp. Teor. Fiz.* **68**, 1724 (1975) [*Sov. Phys. JETP* **41**, 865 (1975)].
- [13] J. O. Phelps, J. E. Solomon, D. F. Korff, C. C. Lin, and E. T. P. Lee, *Phys. Rev. A* **20**, 1418 (1979).
- [14] H. R. J. Walters, *J. Phys. B* **6**, 1003 (1973).
- [15] H. R. J. Walters, *J. Phys. B* **9**, 227 (1976).
- [16] J. V. Kennedy, V. P. Myerscough, and M. R. C. McDowell, *J. Phys. B* **10**, 3759 (1977).
- [17] T. S. Stein, M. S. Dababneh, W. E. Kauppila, C. K. Kwan, and Y. J. Wan, in *Atomic Physics with Positrons*, Vol. 169 of *NATO Advanced Study Institute, Series B: Physics*, edited by J. W. Humberston and E. A. G. Armour (Plenum, New York, 1987), pp. 251–263.
- [18] T. T. Gien, *J. Phys. B* **22**, L129 (1989).
- [19] R. E. Collins, B. Bederson, and Goldstein (unpublished).
- [20] E. M. Karule (unpublished).
- [21] E. M. Karule and R. K. Peterkop (unpublished).
- [22] R. B. Brode, *Phys. Rev.* **34**, 673 (1929).
- [23] E. Clementi and C. Roetti, *At. Data Nucl. Data Tables* **14**, 177 (1974).
- [24] A. Hibbert, *Comput. Phys. Commun.* **9**, 141 (1975).
- [25] W. L. Wiese, M. W. Smith, and B. H. Miles, *Atomic Transition Probabilities*, Natl. Bur. Stand. (U.S.) Circ. No. 422 (U.S. GPO, Washington, D.C., 1969), Vol. 3.
- [26] C. E. Moore, *Atomic Energy Levels*, Natl. Bur. Stand. (U.S.) Circ. No. 467 (U.S. GPO, Washington, D.C., 1949), Vol. 1.
- [27] K. A. Berrington, P. G. Burke, W. D. Robb, M. Le Dourneuf, K. T. Taylor, and V. Ky Lan, *Comput. Phys. Commun.* **14**, 367 (1978).
- [28] Yu P. Korchevoi and A. M. Prozonki, *Zh. Eksp. Teor. Fiz.* **51**, 1617 (1967) [*Sov. Phys.—JETP* **24**, 1089 (1967)].
- [29] R. H. McFarland and J. D. Kinney, *Phys. Rev.* **137**, 1058 (1965).
- [30] A. Z. Msesane, *Phys. Rev. A* **37**, 1787 (1988).
- [31] D. L. Moores, *J. Phys. B* **9**, 1329 (1976).
- [32] D. L. Moores and D. Norcross, *J. Phys. B* **5**, 1482 (1972).
- [33] P. Awuah and A. Z. Msezane, in *Abstracts of Papers, Proceedings of the Seventeenth International Conference on the Physics of Electronic and Atomic Collisions, Brisbane, Australia, 1991*, edited by I. E. McCarthy (Griffith University, Brisbane, 1991), p. 155.